Turk J Chem
36 (2012) , 69 – 79.

doi:10.3906/kim-1106-61

Synthesis and characterization of transition metal coordination polymers derived from 1,4-benzenedicarboxylate and certain azoles

Aref A. M. ALY*, **Mahmoud A. GHANDOUR, Maged S. AL-FAKEH**
Department of Chemistry, Faculty of Science, Assiut University, Assiut-EGYPT
e-mail: aref_20002001@yahoo.com

Received: 25.06.2011

A series of coordination polymers of the general formula $\{[M(BDC)(azoles)(H_2O)_m].xH_2O\}_n$ (where M = Co(II), Ni(II), and Cu(II); BDC = 1,4-benzenedicarboxylate; azoles = 2-aminobenzothiazole, 2-aminothiazole, and 2-amino-4-methyl-thiazole; m = 0 or 1; and x = 1 or 2) were prepared and characterized. The complexes were characterized based on elemental analysis, infrared and electronic spectral studies, magnetic measurements, molar conductance, thermal analysis, X-ray diffraction, scanning electron microscopy, and biological activity. Thermogravimetry, derivative thermogravimetry, and differential thermal analysis were used to study the thermal decomposition of the complexes. The kinetic parameters were calculated making use of the Coats-Redfern and Horowitz-Metzger equations.

Key Words: Coordination polymers, spectral studies, biological activity

Introduction

1,4-Benzenedicarboxylic acid and its metal complexes have been a subject of interest in numerous studies because of their chemical and biological activities. Aromatic polycarboxylates, such as benzenedicarboxylate, have been used to construct coordination frameworks[1] by direct interaction with metal ions to form discrete polynuclear 1-, 2-, and 3-D coordination networks[2,3] in a variety of coordination modes. 1,4-Benzenedicarboxylate (BDC) exhibits a variety of bridging modes and a strong tendency to form large, tightly bound metal cluster aggregates. Recently, mixed-linker systems of both carboxylates and other ligands have proven to be effective in the preparation of novel coordination polymers.[4–9] A number of publications have dealt with the investigation

*Corresponding author

of mixed ligand complexes comprising BDC and nitrogen donors.[10−11] Thiazoles represent a very interesting class of compounds because of their pharmaceutical, analytical, and industrial applications.[12] In this paper, the synthesis and characterization of Co(II), Ni(II), and Cu(II) complexes containing 1,4-benzenedicarboxylate and azole ligands are described. The structures of the ligands are depicted in Figure 1.

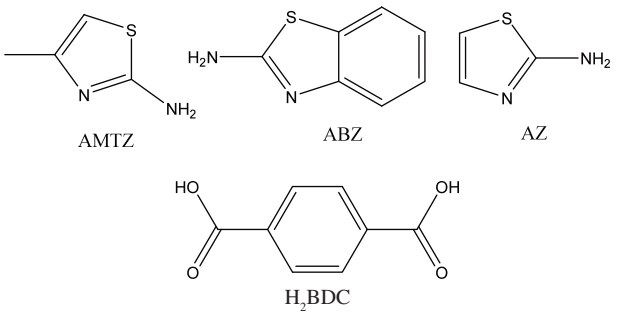

Figure 1. Structures of the ligands.

Experimental

All chemicals were of analytical grade. 1,4-Benzenedicarboxylic acid,

2-aminobenzothiazole, 2-aminothiazole, and 2-amino-4-methyl-thiazole were of E. Merck grade and were used without further purification.

Preparation of the complexes

Preparation of the mixed ligand complexes of 1,4-benzenedicarboxylic acid and azoles 2-aminobenzothiazole (ABZ), 2-aminothiazole (AZ), and 2-amino-4-methyl-thiazole (AMTZ) with Co(II), Ni(II), and Cu(II) followed essentially the same procedure. $[Co(BDC)(ABZ)(H_2O)].H_2O$ is typical. To an ethanolic solution (15 mL) of Co(II) chloride (0.57 g, 2.4 mmol), a solution of BDC (0.4 g of H_2BDC in 15 mL of 0.1 M NaOH, 2.4 mmol) was added dropwise with stirring, and then a solution of ABZ (0.362 g in 15 mL of ethanol, 2.4 mmol) was added to the mixture. The mixture was refluxed and then cooled to room temperature. A light-pink precipitate separated, which was filtered, washed with distilled water and EtOH, and dried over anhydrous $CaCl_2$.

Physical measurements

Stoichiometric analyses (C, H, N, S) were performed using a Vario EL elemental analyzer. The infrared (IR) spectra were recorded on a Shimadzu IR-470 spectrophotometer and the electronic spectra were obtained using a Shimadzu UV-2101 PC spectrophotometer. Thermal studies were carried out in dynamic air on a Shimadzu DTG 60-H thermal analyzer at a heating rate of 10 °C min^{-1}. Magnetic moments of the prepared complexes were measured at room temperature using a magnetic susceptibility balance of the type MSB-Auto. Molar susceptibilities were corrected for diamagnetism of the component atoms by use of the Pascal's constants. The calibrant used was $Hg[Co(SCN)_4]$.

Results and discussion

The complexes were prepared by the reaction of 1,4-benzenedicarboxylic acid (neutralized with NaOH), metal chlorides, and ABZ, AZ, and AMTZ (dissolved in EtOH). The prepared complexes were found to react in a molar ratio of 1:1:1 of metal, BDC, and azoles to yield the corresponding coordination polymers according to the following equation.

$$MCl_2 + Na_2BDC + azoleEtOH/H_2O \rightarrow \{[M(BDC)(azole)(H_2O)_m].xH_2O\}_n + 2NaCl \qquad (1)$$

$$m = 0 \text{ or } 1; \qquad x = 0, 1, \text{ or } 2.$$

The complexes are air-stable; they are insoluble in common organic solvents but partially soluble in DMF and DMSO. The conductivity values, measured in DMSO at room temperature, fall within the range for nonelectrolytes.[13] The compositions of the complexes are supported by the elemental analysis provided in Table 1.

Table 1. Colors, elemental analyses, and melting points of the complexes.

Complex	Color	Found (Calcd. %)				Mp, °C (decomp.)
		C	H	N	S	
$\{[Co(BDC)(ABZ)(H_2O)].H_2O\}_n$ **1**	Pink	45.92 (44.04)	3.47 (3.93)	6.60 (6.84)	6.80 (7.83)	207
$\{[Co(BDC)(AZ)(H_2O)].H_2O\}_n$ **2**	Pink	37.78 (36.77)	3.43 (3.36)	8.06 (7.79)	8.51 (8.92)	213
$[Ni(BDC)(ABZ)(H_2O)].H_2O\}_n$ **3**	Light green	45.09 (44.04)	3.49 (3.44)	6.00 (6.84)	6.22 (7.83)	218
$\{[Cu(BDC)(ABZ)]\}_n$ **4**	Light blue	47.47 (47.68)	2.86 (2.66)	6.99 (7.41)	7.60 (8.48)	242
$\{[Cu(BDC)(AZ)(H_2O)].H_2O\}_n$ **5**	Greenish-blue	35.52 (36.31)	2.75 (3.32)	7.87 (7.69)	8.95 (8.81)	224
$\{[Cu(BDC)(AMTZ)(H_2O)].2H_2O\}_n$ **6**	Greenish-blue	35.76 (36.40)	3.54 (4.06)	7.14 (7.07)	8.02 (8.10)	225

IR spectra

The main IR frequencies can be seen in Table 2. The IR spectra of the prepared compounds show 2 bands in the ranges of 1552-1572 and 1374-1380 cm^{-1}, characteristic of the asymmetric and symmetric stretching vibrations of the carboxylic groups of BDC coordinated to the metal center. The separation value $\Delta\upsilon \leq 192$ cm^{-1} indicates a bidentate mode of coordination for the carboxylate group.[14] Furthermore, it was found that the CSC band of the azoles occurred at approximately 740 cm^{-1} and was almost unchanged in the respective complexes compared to the free ligands, indicating that the thiazole-S is not involved in the bonding.[15] The stretching vibration of νC=N for azoles incorporated in complexes **1**, **2**, **3**, **5**, and **6** underwent no appreciable shift in comparison with the ligands, but in complex **4**, a frequency of 1626 cm^{-1} was observed compared to the parent, free ABZ, at 1640 cm^{-1}.[16] Moreover, the stretching vibration of the amino group in free ABZ, observed

at 3220 cm^{-1}, shifted to a lower wave number and appeared in the range of 3150-3200 cm^{-1} in the complexes, suggesting coordination of the amino nitrogen to the metal(II) ions.[17] The bands at 3480-3505 cm^{-1} in the spectra of complexes **1**, **2**, **3**, **5**, and **6** were assigned to the νOH of water of crystallization,[18] whereas the νOH stretching vibrations of the coordinated water molecules were located in the range of 3390-3410 cm^{-1} for these complexes.[19] Metal-oxygen and metal-nitrogen bonding was manifested by the appearance of a band in the 510-524 and 405-420 cm^{-1} regions, respectively.

Table 2. Infrared spectral data of mixed ligand complexes.

Compound	$\nu(NH_2)$	ν(COO) asym.	ν(COO) sym.	$\nu\Delta$	ν(C=N)	ν(C-S)	ν(OH) coord.	ν(OH) lattice	ν(M-N)	ν(M-O)
1	3180	1560	1378	182	1638	744	3390	3498	412	510
2	3150	1564	1374	190	1620	742	3400	3490	410	518
3	3180	1565	1380	185	1640	740	3410	3505	418	510
4	3200	1572	1380	192	1626	740	-	-	410	520
5	3180	1552	1376	176	1618	736	3595	3500	420	524
6	3180	1566	1378	188	1618	738	3480	3480	405	518

Electronic spectra and magnetic moments

The UV-Vis spectra of the complexes were recorded in DMSO (Table 3). The spectra displayed 2 distinct bands in the ranges of 36,363-38,819 and 23,866-30,769 cm^{-1}, attributed to $\pi \rightarrow \pi^*$ and n$\rightarrow \pi^*$ transitions within the BDC and azole moieties,[15,18] respectively. In the visible spectra, there were characteristic bands attributed to the d-d transitions in the Co(II), Ni(II), and Cu(II) complexes typical of octahedral structures (Figures 2 and 3). Thus, Co(II) complexes **1** and **2** exhibited a d-d band in the range of 15,181-17,825 cm^{-1} corresponding to the transition $^4T_{1g} \rightarrow ^4T_{1g}$. The Ni(II) complex exhibited a band at 23,866 cm^{-1}, which can be tentatively assigned to the $^3T_1(F) \rightarrow {}^3T_2(F)$ transition.[20] The electronic spectra of Cu(II) complexes **4**, **5**, and **6** exhibited broad bands centered at 13,675, 14,877, and 16,132 cm^{-1}, respectively, corresponding to the $^2B_1g \rightarrow {}^2A_1g$ transition and indicative of a distorted octahedral geometry around Cu(II).[15] Additionally, the magnetic moments of the compounds were measured, and it was found that Co(II) complexes **1** and **2** had magnetic moments in the range of 4.2-5.07 BM, typical for octahedral complexes,[15] whereas Ni(II) complex **3** had a magnetic moment value of 2.87 BM, closely related to the value expected for octahedral complexes. The distorted octahedral geometry around Cu(II) was confirmed by magnetic moment values in the range of 2.04-2.06 BM. These values are typical of magnetically dilute complexes, in which the individual Cu(II) ions are separated from each other with no intermolecular magnetic interaction.[21]

Thermal studies

The thermal decomposition of the coordination polymers was investigated in dynamic air from ambient temperature to 750 °C (Table 4). As a representative example, the thermal behavior of Ni complex **3** is described. The

thermal analysis curve of the complex showed 5 decomposition stages. The first stage corresponds to the release of 2 water molecules, the lattice and the coordinated molecules (calcd. 8.80%, found 8.63%). The elimination of both the lattice and coordinated water molecules may indicate that their bonding to the Ni(II) center is of the ion-dipole type. The derivative thermogravimetry (DTG) curve displayed this step at 196 °C, and an endothermic peak appeared at 201 °C in the differential thermal analysis (DTA). The second, third, fourth, and fifth steps correspond to the decomposition of ABZ and BDC ligands. The final product was identified on the basis of mass loss considered as NiO (calcd. 18.49%, found 18.73%) (Figure 4). The scheme represents the decomposition of complex **3**.

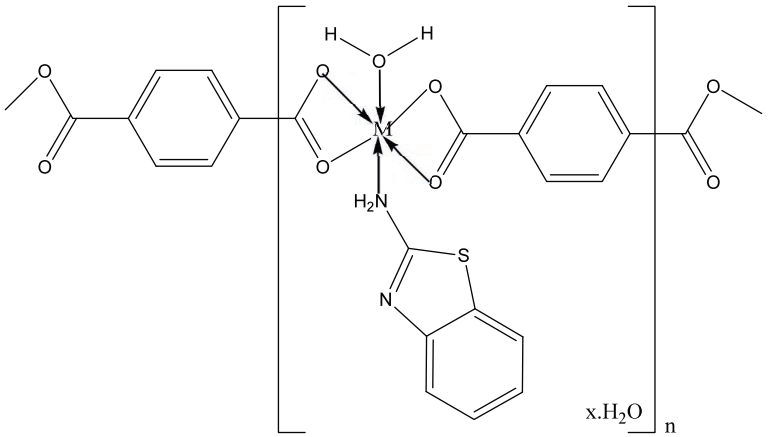

Figure 2. Structure of complexes $\{[M(BDC)(ABZ)(H_2O)].xH_2O\}_n$, M = Co(II) and Ni(II), x = 1 or 2.

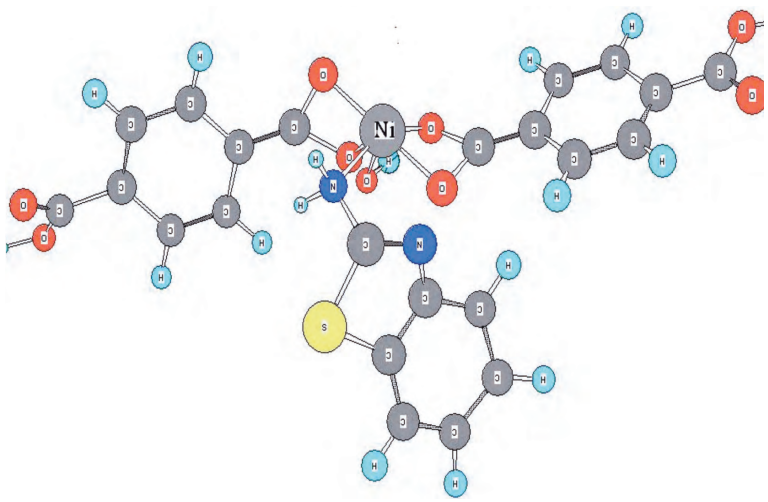

Figure 3. A perspective view of the complete coordination around Ni.

Table 3. Electronic spectral data of the complexes.

Compound	ν_{max} (cm^{-1})	Assignment	μ_{eff} BM
1	17,825 24,330 38,819	$^4T_{1g} \rightarrow {}^4T_{1g}$ n-π* transition π-π* transition	4.2
2	15,181 23,866 38,759	$^4T_{1g} \rightarrow {}^4T_{1g}$ n-π* transition π-π* transition	5.07
3	23,866 28,571 37,216	$^3T_2(F) \rightarrow {}^3T_1(F)$ n-π* transition π-π* transition	2.87
4	13,675 30,769 36,363	d-d transition n-π* transition π-π* transition	2.05
5	14,877 28,571 38,022	d-d transition n-π* transition π-π* transition	2.06
6	16,132 28,089 38,167	d-d transition n-π* transition π-π* transition	2.04

Table 4. Thermal decomposition data of the complexes in dynamic air.

Compound	Step	TG/DTG			Mass loss (%)
		T_i	T_m	T_f	
1	1	66	172	215	8.46
	2	216	227	241	13.26
	3	243	274	335	11.62
	4	336	466	751	47.35
2	1	104	181	227	11.79
	2	228	452	750	55.13
3	1	65	169	183	8.63
	2	184	207	224	9.70
	3	225	238	262	6.04
	4	263	303	320	14.38
	5	322	560	751	41.21
4	1	146	261	274	9.00
	2	275	286	298	29.19
	3	299	352	750	41.11
5	1	75	155	277	9.21
	2	279	327	750	69.03

T_i = Initial temperature, T_m = maximum temperature, T_f = final temperature.

Kinetic analysis

Nonisothermal kinetic analysis of the complexes was carried out by applying 2 different procedures: the Coats-Redfern[22] and the Horowitz-Metzger[23] methods.

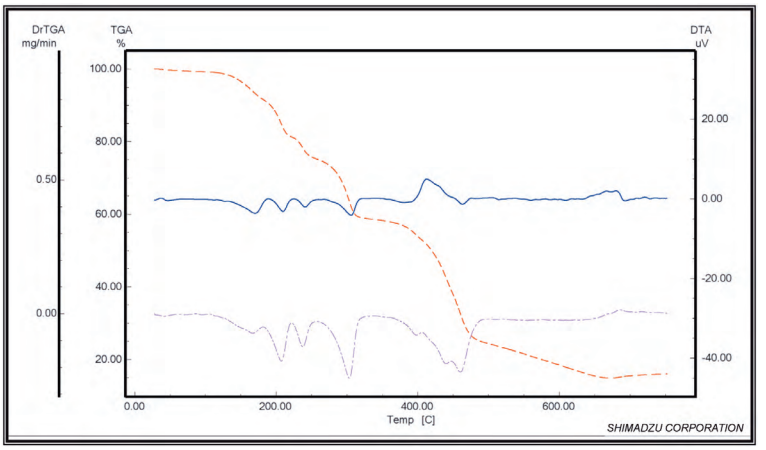

Figure 4. TG, DTG, and DTA thermal analysis curves of compound **3** in dynamic air.

$$[Ni(BDC)(ABZ)(H_2O)].H_2O \xrightarrow[\text{First step}]{65\text{-}183\ ^\circ C} [Ni(BDC)(ABZ)] + 2H_2O$$

$$[Ni(BDC)(ABZ)] \xrightarrow{184\text{-}751\ ^\circ C} \text{Decomposition products + NiO}$$

(in dynamic air)

Scheme.

Coats-Redfern equation

$$ln[1-(1-\alpha)^{1-n}/(1-n)T^2] = M/T + B \text{ for } n \neq 1 \quad (2)$$

$$\ln[-\ln(1-\alpha)/T^2] = M/T + B \text{ for } n = 1 \quad (3)$$

Here, α is the fraction of material decomposed, n is the order of the decomposition reaction, and M = E/R and B = ZR/ΦE, where E, R, Z, and Φ are the activation energy, gas constant, preexponential factor, and heating rate, respectively.

Horowitz-Metzger equation

$$\ln[1-(1-\alpha)^{1-n}/1-n] = \ln ZRT_s^2/\Phi E - E/RT_s + E\theta/RT_s^2 \text{ for } n \neq 1 \quad (4)$$

$$\ln[-\ln(1-\alpha)] = E\theta/RT_s^2 \text{ for } n = 1 \quad (5)$$

Here, $\theta = T - T_s$, and T_s is the temperature at the DTG peak.

The correlation coefficient r was computed using the least squares method for Eqs. (2), (3), (4), and (5). Linear curves were drawn for different values of n, ranging from 0 to 2. The value of n that gave the best fit was chosen as the order parameter for the decomposition stage of interest. The kinetic parameters were calculated from the plots of the left-hand side of Eqs. (2) and (3) against 1/T and against θ for Eqs. (4) and (5). The kinetic parameters were calculated according to the above 2 methods and are cited in Table 5. Figure 5 illustrates the Coats-Redfern plots of compound **1** for the first step in dynamic air.

Table 5. Kinetic parameters for the first step of thermal decomposition of the complexes in dynamic air.

Compound	Step	Coats-Redfern equation			Horowitz-Metzger equation		
		r	n	E	r	n	E
1	1	1	0.66	22	0.9983	0.66	30
2	1	1	1.00	44	1	1.00	51
3	1	0.9960	2.00	123	1	2.00	125

E in kJ mol^{-1}.

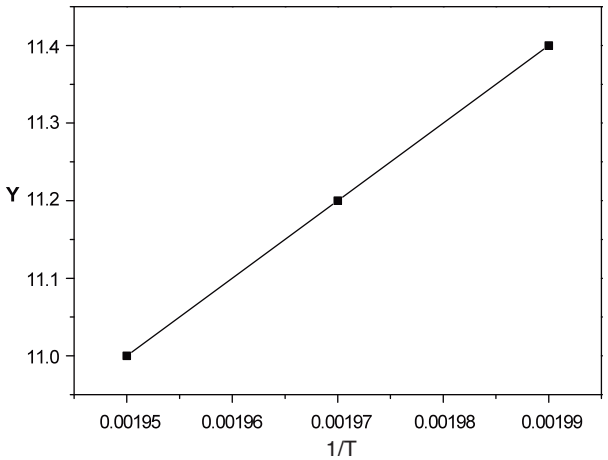

Figure 5. Coats-Redfern plots for the first step of compound **1** in dynamic air, where $Y = \ln[1-(1-\alpha)^{1-n}/(1-\alpha)T^2]$ for $n \neq 1$.

X-ray powder diffraction

The X-ray powder diffraction patterns of $\{[Cu(BDC)(ABZ)]\}_n$ and its CuO residue after decomposition were recorded. The crystal lattice parameters were computed with the aid of the computer program TREOR. The crystal data of the complex belong to the triclinic crystal system, while the residue is monoclinic. The Scherrer equation was applied to estimate the particle size of the compound and its residue:

$$D = K\lambda/\beta\cos\theta, \tag{6}$$

where K is the shape factor, λ is the X-ray wavelength (typically 1.54 Å), β is the line broadening at half the maximum intensity in radians, θ is the Bragg angle, and D is the mean size of the ordered (crystalline) domains, which may be smaller than or equal to the grain size. The crystal data, together with the average particle sizes, are given in Table 6. The broadening observed in the X-ray powder diffraction patterns of the complex and CuO indicates the nanosized nature of the 2 compounds. Figure 6 illustrates the nanostructure of the copper complex. The particles are almost spherical in shape.

Table 6. The crystal data of complex **4** and the residue CuO.

Compound	a (Å)	b (Å)	c (Å)	α	β	λ	Volume of unit cell (Å)	Crystal system	Particle size (nm)
[Cu(BDC)(ABZ)]	9.46	14.34	17.23	93.59	46.68	129.57	976.74	Triclinic	21
CuO	4.71	3.49	5.19	90.00	99.87	90.00	182.95	Monoclinic	15

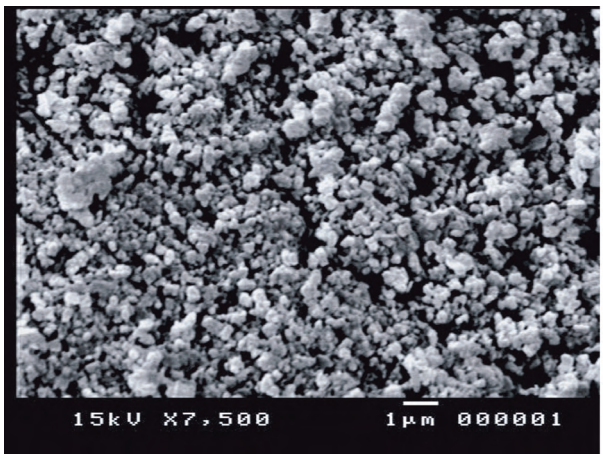

Figure 6. SEM of compound **4**.

Scanning electron microscopy

The scanning electron microscopy (SEM) results of compound **4** as a representative example are given in Figure 6. This compound is crystalline, and the size of the particles is indicated under Figure 6 in micrometers.

Microbiological screening

1,4-Benzenedicarboxylic acid and ternary complexes **2-6** were tested against some bacteria and fungi. The antimicrobial activity of the synthesized compounds was tested against 5 bacterial and 6 fungal species (Table 7).

Table 7. Microbiological screening of the complexes.

Compound	B. cereus (G+ve)	S. aureus (G+ve)	S. marcescens (G-ve)	E. coli (G-ve)	P. aerugin osa (G-ve)	T. rubrum	A. flavus	C. albicans	F. oxysporum	G. candidum	S. brevicaulis
2	12	8	13	11	13	16	0	0	18	16	0
3	8	11	14	10	0	10	10	14	35	11	12
4	8	14	16	13	10	8	8	10	10	11	10
6	0	8	12	0	0	0	0	0	0	0	0

Figure 7 illustrates that compound **3** was highly effective against the tested microbes, especially against *Fusarium oxysporum*, a plant pathogen causing wilt disease. The toxic action of the prepared complexes against the growth of bacteria and fungi was studied. The bacterial and fungal action may be due to the following.

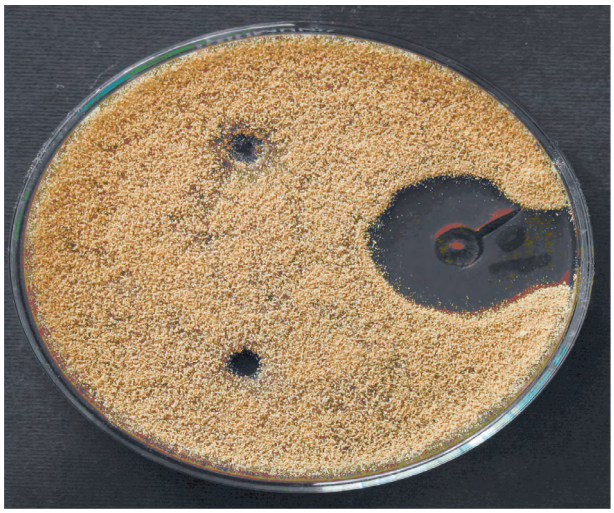

Figure 7. Microbiological screening of compound **3** against *F. oxysporum*.

a) Thiols, which are the vital constituents in the living cells and have reduction potential for disulfide forms at or below –200 mV, may be oxidized by the studied metal complexes.

b) The complexes may cause disturbances in the respiration process.

c) The presence of the (C=S) group in the azole complexes might cause the action.[24–29]

Acknowledgment

A. A. M. Aly would like to thank the Alexander von Humboldt Foundation for donating the magnetic susceptibility balance of the type MSB-Auto.

References

1. Steiner, T. *Angew. Chem. Int. Ed. Engl.* **2002**, *41*, 48-52.
2. Swan, S. *Environmental Research* **2008**, *108*, 177-181.
3. Aullon, G.; Bellamy, D.; Orpen, A.; Brammer, L.; Bruton, A. *Chem. Comm.* **1998**, 653.
4. Pyykko, P. *Chem. Rev.* **1997**, *97*, 597-601.
5. Clegg, W. *J. Coord. Chem.* **2004**, *1*, 579-582.
6. Carlucci, L.; Ciani, G.; Proserpio, D. *Coord. Chem. Rev.* **2003**, *246*, 247.
7. Holman, K.; Hammud, H.; Isber, S.; Tabbal, M. *Polyhedron* **2005**, *24*, 221-225.
8. Choi, H.; Suh, M. *Inorg. Chem.* **1999**, *38*, 6309-6312.
9. Robin, A.; Fromm, K.; Goesmann, H.; Bernardinelli, G. *Cryst. Eng. Commun.* **2003**, *5*, 405-408.
10. Li, W.; Li, M.; Shao, X.; Zhu, S. *Inorg. Chem. Comm.* **2007**, *10*, 753-757.
11. Yoo, H.; Lim, J.; Kang, J.; Koh, E.; Hong, C. *Polyhedron* **2007**, *26*, 4383-4386.

12. Agarwal, N.; Kumar, K. *Ind. J. Het. Chem.* **1997**, *6*, 291-294.
13. Geary, W. *Coord. Chem. Rev.* **1971**, *7*, 81-84.
14. Rogan, J.; Poleti, D.; Karanovic, L.; Bogdanovic, G.; Spasojevic-de Bire, A.; Petrovic, D. M. *Polyhedron* **2000**, *19*, 1415-1417.
15. Maurya, R. C.; Verma, R.; Singh, H. *Synth. React. Inorg. Metal-Org. Chem.* **2003**, *33*, 1063-1066.
16. Lane, T. J.; Nakagawa, I.; Walter, J. L.; Kandathil, A. J. *Inorg. Chem.* **1962**, *1*, 267-270.
17. Aly, A. A. M.; El-Maligy, M. S.; Zidan, A. S.; El-Shabasy, M. *Anal. Quim.* **1990**, *86*, 19-23.
18. Bravo, A.; Anacona, J. R. *Trans. Met. Chem.* **2001**, *26*, 20-25.
19. Rakha, T. H. *Synth. React. Inorg. Met.-Org. Chem.* **2000**, *30*, 205-208.
20. Lever, A. B. P. *Inorganic Electronic Spectroscopy*, 2nd edition, Elsevier, Amsterdam, 1984.
21. (a) Paulovicova A.; El-Ayaan, U; Fukuda, Y *Inorg. Chim. Acta* **2001**, *321*, 5662. (b) Hathaway B. J; Billing D. E *Coord. Chem. Rev.* **1970**, *5*, 143-207.
22. Coats, A. W.; Redfern, J. P. *Nature* **1964**, *20*, 68-73.
23. Horowitz, H.; Metzger, G. *Anal. Chem.* **1963**, *350*, 1464-1467.
24. Ferguson, J. *Proc. Roy. Soc. Lond. B* **1939**, *127*, 387-404.
25. Horsfall, G. *Principles of Fungicidal Action*, Chronica Botanica, Waltham, MA 1956.
26. Owens, G. *Contrib. Boyce Thompson Inst.* **1953**, *17*, 221-225.
27. McCallan, S. E. A. In *Proceedings of the Plant Protection Conference 1956*, Butterworths, London, 1957.
28. Miller, O.; McCallan, S. E. A. *J. Agr. Food. Chem.* **1957**, *5*, 116-122.
29. Anjaneyulu, Y. *Synth. React. Inorg. Met.-Org. Chem.* **1986**, *16*, 257-260.